Cureus Journal of Engineering

Open Access Original Article

On the Electrical Properties of Chitosan Doped with Different Lanthanide Oxides: Influence of Ion Size and Surface Roughness

Received 10/16/2024
Review began 11/24/2024
Review ended 04/29/2025
Published 05/16/2025

DOI: https://doi.org/10.7759/s44388-024-00475-w

Kabiriyel J. [1] , Padma M.J. [2] , Jeyanthi R. [2] , Shanmugaprakash R. [2] , Chinnan Raja Mohan [2]

1. Department of Physics, Mary Matha College of Arts and Science, Periyakulam, IND 2. Department of Physics, The Gandhigram Rural Institute (Deemed to be University), Dindigul, IND

Corresponding authors: Kabiriyel J., jerigabrielguru@gmail.com, Padma M.J., padmarajasekaran0801@gmail.com, Jeyanthi R., jeyanthidinesh01@gmail.com, Shanmugaprakash R., shannprakas@gmail.com, Chinnan Raja Mohan, crmohan.gru@gmail.com

Abstract

This study examines the effect of ion-sized ion size of lanthanide oxide (LO) involved with chitosan matrix and surface roughness on the electrical properties of chitosan thin films. Chitosan films were designed using a solution casting method with various LOs (CeO_2, Nd_2O_3, Sm_2O_3, Eu_2O_3, Gd_2O_3, Dy_2O_3, and Ho_2O_3). Chemical interactions and structural changes in films were analyzed using the Fourier-Transform Infrared Spectroscopy, which confirmed the successful inclusion of LOs in chitosan matrix. Photoluminescence (PL) learned increased optical properties in LO-doped films, with the samarium-doped film performing the highest PL intensity. Scanning electron microscopy and Atomic force microscopy (AFM) were employed to study the morphological characteristics and surface roughness of films. AFM analysis showed variation in surface roughness based on LO dopant, including 28.9 Nm for Dy_2O_3-doped chitosan to 264 nm for Ho_2O_3-doped chitosan. Electrical conductivity measurement using a Keithley source meter demonstrated a connection between surface roughness and conductivity, aligning with the Fishman and Calecki model. Gd_2O_3- and Ho_2O_3-doped samples performed the highest conductivity among LO-doped films. These findings suggest that LO doping can be used to tailor surface properties and increase the electrical conductivity of chitosan films, to open new possibilities for their application in bioelectronics, environmental treatment, and advanced material science.

Categories: Polymer Science and Engineering
Keywords: chitosan, lanthanide oxide, surface roughness, conductivity, polymer composite

Introduction

The research on chitosan-based biopolymers [1] has increased significantly due to their unique properties of biodegradability, biocompatibility, antibacterial activity [2,3], and non-toxicity. The materials are versatile by controlling their degree of deacetylation, self-similar property [4], ion size [5], and molecular weight, making possible uses in environmental remediation, energy storage, and biomedical devices [6,7]. The versatility of chitosan-based materials has resulted in their investigation in various areas of research, ranging from drug delivery systems, tissue engineering scaffolds, to water purification technologies [8-10]. With the addition of rare-earth elements, primarily lanthanide oxides (LOs), chitosan polymers have had their applications further diversified, particularly for fluoride removal and oil adsorption [11-13]. Their incorporation has led to new ways of increasing the functionality of chitosan-derived materials so that advanced composites with better mechanical, optical, and chemical characteristics can be designed. The novel electronic structure of lanthanides is responsible for the development of complexes with chitosan, leading to more efficient adsorbents and catalytic materials [14-18].

Physical, chemical, and mechanical properties of chitosan can be controlled by altering its degree of deacetylation and molecular weight [19-21], rendering it a flexible material suitable for use in different applications such as environmental remediation, energy storage, and biomedical devices [22]. In addition, materials doped with rare earth have drawn interest due to their potential use in dielectric resonators [23,24] and Light Emitting Diodes (LEDs) [25,26]. With these benefits, LO-doped chitosan polymers have been investigated for fluoride removal, oil adsorption, and other environmental remediation methods. It has also been investigated for therapeutic applications, wound healing, and other biomedical applications by Hassannejad [27], Blasse [28], and Zhang [29]. Although there have been studies of the electrical properties of chitosan-based composites, few have examined variations in ion size [19], doping by ammonium salts [5], or acid effects on dissolving chitosan [22]. Yet, its influence on electrical conductivity has long remained unexplored. More recently, evidence emerged that the conductivity of thin films can be appreciably influenced by surface roughness, especially when film thickness is comparable with the average electron free path [30-32].

Current studies have aimed at improving the electrical characteristics of chitosan-based composites by doping with different LOs and other nanoparticles. These investigations have shown considerable enhancement in dielectric behavior, AC conductivity, and piezoelectric properties, which depend on the type of dopant and the surface morphology formed. One study of chitosan-lanthanum oxide (La_2O_3) nanocomposites showed that adding La_2O_3 nanoparticles to the chitosan matrix increases the dielectric constant and AC conductivity. This is due to the interaction between the NH_2 groups of chitosan and the La^{3+} ions, allowing improved charge transport mechanisms [33]. Yet another study investigated the microstructure and physical properties of green piezoelectric composite thin films composed of chitosan and Ln_2O_3-doped $Na_{0.5}Bi_{0.5}TiO_3$-$BaTiO_3$ nanoparticles. The researchers discovered that incorporating lanthanide-doped nanoparticles into the chitosan matrix improved dielectric characteristics and piezoelectric response. The surface morphology analysis revealed enhanced roughness and porosity, which contributed to these enhanced electrical characteristics [34]. Though not employing LOs, studies involving chitosan-ZnO nanocomposites have also been informative. Such composites showed enhanced dielectric, mechanical, and piezoelectric characteristics as a result of the homogeneous dispersion of ZnO nanoparticles in the chitosan matrix. The increased surface roughness seen in these composites is said to improve the piezoelectric performance [35]. In the same way, chitosan-silver (Chs-Ag) composites studies proved that the addition of silver nanoparticles largely increases the dielectric constant and AC conductivity of chitosan. The developments are concentration dependent, with enhanced electrical performance realized at higher silver concentrations [36]. Research on chitosan-based thin films involving titanium oxide and hematite nanoparticles showed promise in optoelectronic applications. Inclusion of the nanoparticles changed the surface morphology and the dielectric and optoelectronic properties [37]. Research on chitosan-nickel oxide (NiO) nanocomposites has identified remarkable improvement in dielectric properties. Introduction of NiO nanoparticles into the matrix of chitosan provided a composite material that had conductivity 1.4×10^{-2} S cm^{-1} with 4 wt% of NiO content. This enhancement is due to the interaction of chitosan functional groups and NiO nanoparticles, allowing enhanced charge transport mechanisms. The research also noted that the activation energies of the composite films reduced as the content of NiO increased, showing enhanced electrical performance [38].

Although numerous studies have investigated other properties of chitosan-based composites, such as the influence of ion size, ammonium salt doping, and acid dissolution, there is still a large gap in the knowledge regarding the correlation between surface morphology and electrical conductivity in these materials. This inadequate knowledge has disrupted adaptation of chitosan-based materials for targeted applications, especially in the field of bioelectronic and smart materials. To fill this knowledge interval, the current research uses a multidimensional approach that uses a multidimensional approach that integrates different LOs with atomic force microscopy (AFM), which is to detect relationships with different oxy. This multidimensional approach allows for detailed observation of nano scale surface topology and their effects on material electrical characteristics, a better all-round of structure-property correlation in such advanced systems. Current research uses simple and elegant functioning such as solutions for smooth film production, as well as methods with accurate-based characteristic such as Fourier-Transform Infrared (FTIR) spectroscopy, photo-luminance studies, and conductivity tests. The solution-casting technique ensures the formation of similar thin films with desired thickness, is important for accurate surface and electrical characteristics. FTIR spectroscopy gives useful information related to chemical interactions between chitosan and LO, while photo-luminance analysis provides insight into electronic structure and energy transfer processes in dopant material.

Materials And Methods

Chitosan with 91% DD (Degree of Deacetylation) was purchased from Pelican Biotech, India, and Analytical grade of formic acid and LO were purchased from Central Drug House, India. Six grams of chitosan were dissolved in 0.066 M formic acid, and this solution was stirred at 900 rpm using a magnetic stirrer for 24 hours. The resulting solution was divided into eight beakers, each containing 50 mL. A 2 mM concentration of various rare earth metal oxides (CeO_2, Nd_2O_3, Sm_2O_3, Eu_2O_3, Gd_2O_3, Dy_2O_3, and Ho_2O_3) was combined with the formate of chitosan as shown in Figure *1*. These mixtures were stirred at 900 rpm with a magnetic stirrer for 2 hours to form a composite. The interaction between chitosan and the different rare earth metal oxides was confirmed using FTIR Spectroscopy within the range of 4000-400 cm^{-1}. As shown in the Table *1*, density was determined using a pre-calibrated density bottle. The refractive index was measured with an Abbe refractometer (R-8 Advance) with an accuracy of 0.001. All measurements were repeated three times to ensure the accuracy of the results. FTIR measurements were made with a PerkinElmer RX1 FTIR spectrophotometer utilizing KBr discs. The morphology was examined using a JEOL JSM-5200 scanning electron microscopy (SEM) operating at 15 kV. The PerkinElmer LS55 fluorescence spectrometer was used to record the PL spectra. AFM analysis was used to determine the morphology and surface roughness of pure and LO-doped chitosan films.

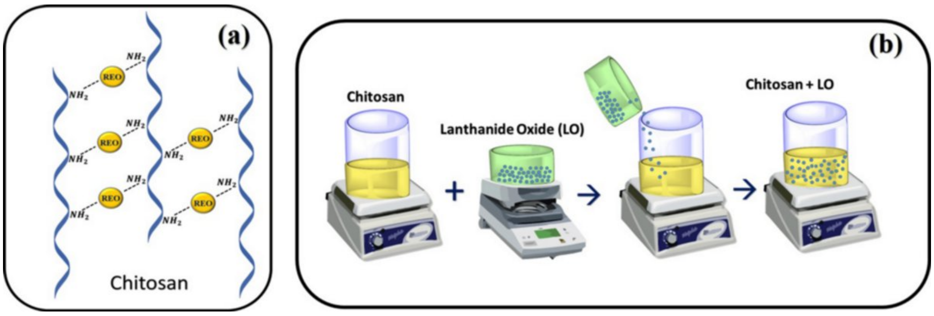

FIGURE 1: (a) Graphical abstract of chitosan-LO; (b) the probable mechanism of chitosan-LO

LO, lanthanide oxide

Chemical compound	Chemical formula	Density (mg/cm^3)	Molar mass (kg/mol)	Ionic radius La^{3+} (nm)
Cerium oxide	CeO_2	0.00722	0.17212	0.122
Neodium oxide	Nd_2O_3	0.00724	0.33648	0.1175
Samarium oxide	Sm_2O_3	0.00834	0.3487	0.114
Europium oxide	Eu_2O_3	0.00742	0.35192	0.112
Gadolinium oxide	Gd_2O_3	0.00707	0.3625	0.1105
Dysprosium oxide	Dy_2O_3	0.00780	0.3730	0.1075
Holmium oxide	Ho_2O_3	0.00841	0.37786	0.1055

TABLE 1: The density, crystal structure, molar mass, atomic mass, and ionic radius of LO

LO, lanthanide oxide

Results

The chitosan-lanthanide oxide (Ch-LO) composite and its functional group were investigated by FTIR spectroscopy characterization and it is depicted in Figure *2a*, which illustrates the characteristic peaks of pure chitosan and Ch-LO composites.

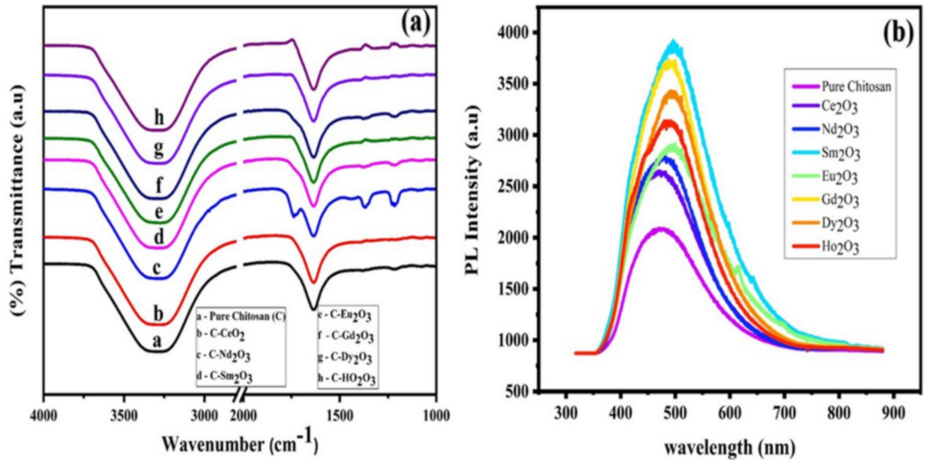

FIGURE 2: (a) FTIR spectra of pure chitosan and Ch-LO and (b) photoluminance of pure chitosan and Ch-LO

FTIR, Fourier-Transform Infrared; Ch-LO, chitosan-lanthanide oxide

The photoluminescence (PL) spectrum of pure chitosan excited at 355 nm is presented in Figure *2b*. The PL intensity of pure chitosan is found to be 480 arbitrary units (a.u.). From the results, it is revealed that doping the chitosan with LOs increases the PL intensity when compared to pure chitosan. The enhancement of PL intensity depends on the type of LO used for doping. Of all the LO-doped chitosan films, the PL intensity of samarium-doped film is substantially greater than those of the other doped films. The extraordinary PL intensity rise for the samarium-doped sample is because the excitation wavelength of samarium-doped sample is just near 370 nm, very close to the used 355 nm excitation in this experiment. The increased PL intensity of doped samples, especially the samarium-doped film, indicates that the addition of LOs to chitosan may enhance its luminescent performance. This may be attributed to energy transfer mechanisms between the lanthanide ions and the chitosan matrix, or the formation of new emission sites in the material. These results have potential relevance for the development of chitosan-based materials with enhanced optical characteristics for diverse uses, including biosensors or optical devices.

Thickness measurement

The prepared solution was cast into the film by solution casting method on the Fluorine-doped Tin Oxide (FTO) substrate. FTO plates having an area of 1 × 1 cm were taken as a substrate. Before forming the film, the substrates were cleaned, dried well, and weighed. Chitosan solution was coated on the FTO substrate by using the solution casting method. All the samples were made to dry at room temperature until completely dry. All samples were again weighed after coating and the mass difference was noted for calculating the thickness of the film using the following relation.

$$t = \Delta m / A \times \rho \quad (1)$$

Where, Δm is the difference of the mass before and after coating, A is the area of the film, ρ is the density of the sample. The results are presented in Table *2*.

S. no	Sample	Density (g/ml)	Thickness (μm)
1	Pure chitosan	0.9930	15.399
2	Chitosan + Ce_2O_3	0.99533	13.422
3	Chitosan + Nd_2O_3	0.99608	14.653
4	Chitosan + Sm_2O_3	0.99674	14.663
5	Chitosan + Eu_2O_3	0.99724	11.578
6	Chitosan + Gd_2O_3	0.99772	16.885
7	Chitosan + Dy_2O_3	0.99822	15.956
8	Chitosan + Ho_2O_3	0.99872	15.482

TABLE 2: The thickness of the various thin films

The SEM (Figure 3) analysis reveals the morphological characteristics of the chitosan LO film. The majority of particles exhibit a spherical morphology, while some elongated particles are observed and appear to be agglomerated. The presence of LO, presumably lanthanide oxides, is evident in the chitosan bio nanocomposite. The Energy Dispersive X-ray Analysis (EDAX) results corroborate the film's purity and confirm the presence of specific rare earth elements, including: Cerium oxide (Ce_2O_3), Neodymium oxide (Nd_2O_3), Samarium oxide (Sm_2O_3), Europium oxide (Eu_2O_3), Gadolinium oxide (Gd_2O_3), Dysprosium oxide (Dy_2O_3), Holmium oxide (Ho_2O_3). The EDAX spectrum exclusively displays these specified rare earth elements, indicating the absence of additional impurities in the film.

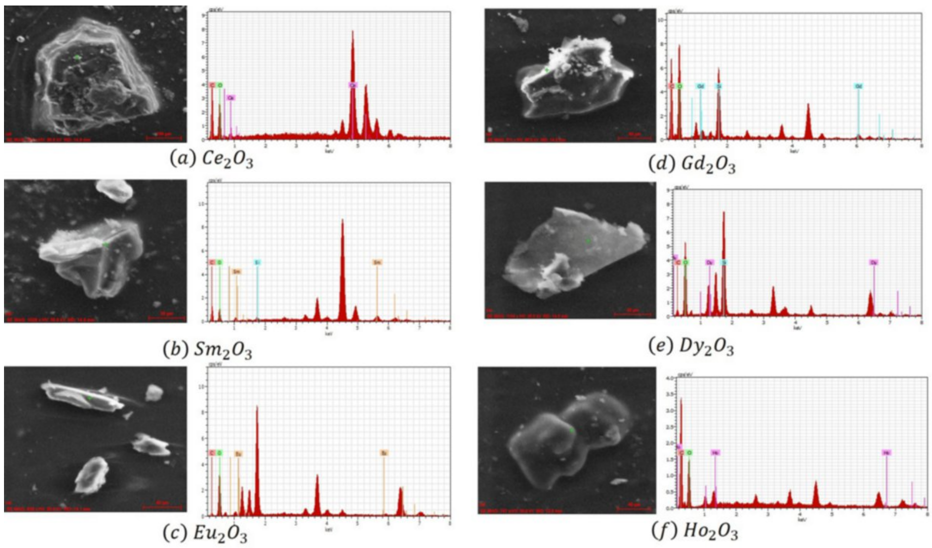

FIGURE 3: SEM and EDAX of chitosan-LO

SEM, scanning electron microscopy; EDAX, Energy Dispersive X-ray Analysis; LO, lanthanide oxide

AFM analysis delivers insightful information about the morphology and surface roughness of pure and LO-doped chitosan films. AFM topography images were obtained for all the samples at scan areas of both 5 × 5 μm and 10 × 10 μm. The AFM images for the pure chitosan film and the LO-doped chitosan films are depicted in Figure 4. These pictures enable a visual comparison of the surface features in the various samples. The changes in the surface topography can be seen, possibly signaling alterations in the structure of the film as a result of the addition of distinct LOs. The visual information is supplemented by Table 3, which gives quantitative measurements of the surface roughness. Table 3 lists the values of the roughness for both the pure chitosan film and the LO-doped films. The roughness parameters listed in Table 3 contain the Average Roughness (Ra) and Root Mean Square (RMS) roughness values. These parameters provide a quantitative estimate of the surface irregularities and can be employed to determine the influence of the incorporation of various LO on the surface properties of the chitosan films. By comparing the values of roughness between the samples, one can ascertain if the addition of LO enhances or reduces the surface roughness of the chitosan films. Such information can be invaluable in the determination of how the doping procedure influences the properties of the film and possibly its functionality in different applications. The integration of AFM visual images and quantitative roughness information gives a complete picture of the surface properties of the chitosan films and enables an accurate comparative analysis between the different samples.

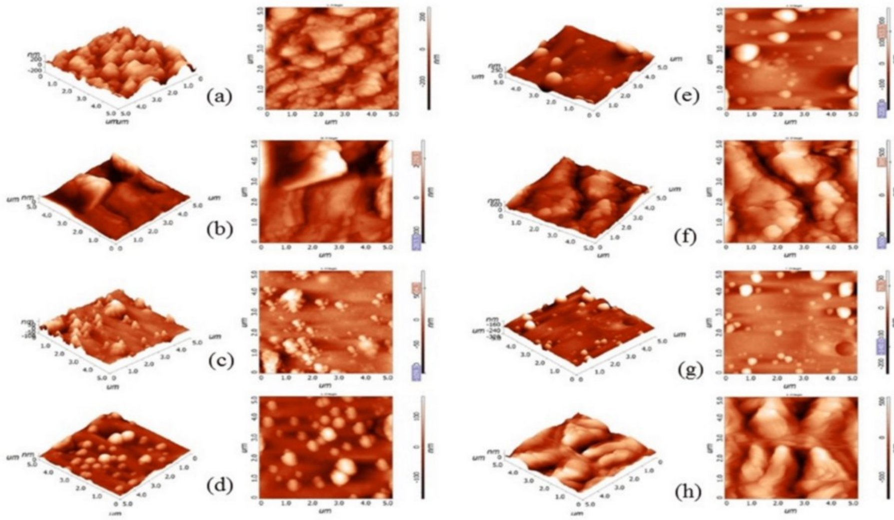

FIGURE 4: AFM of (a) pure chitosan, (b) chitosan-Ce2O3, (c) chitosan-Nd2O3, (d) chitosan-Sm2O3, (e) chitosan-Eu2O3, (f) chitosan-Gd2O3, (g) chitosan-Dy2O3, (h) chitosan-Ho2O3

AFM, atomic force microscopy

S. no	Sample	5 × 5 microns area		10 × 10 microns area	
		RMS roughness (nm)	Average roughness (R_a) (nm)	RMS roughness (nm)	Average roughness(R_a) (nm)
1	Pure chitosan	77.1	62.2	127.1	102.1
2	Chitosan + Ce_2O_3	120.8	88.0	118.0	78.8
3	Chitosan + Nd_2O_3	19.7	13.1	51.3	31.1
4	Chitosan + Sm_2O_3	42.2	30.5	76.9	52.1
5	Chitosan + Eu_2O_3	49.2	32.3	96.9	68.0
6	Chitosan + Gd_2O_3	161.8	128.3	203.7	158.6
7	Chitosan + Dy_2O_3	22.9	13.3	44.3	28.9
8	Chitosan + Ho_2O_3	207.8	164.7	347	264

TABLE 3: Average roughness (Ra) and RMS values of roughness for various chitosan films

RMS, Root Mean Square

The conductivity measurement was carried out by using a Keithley source meter (SCS-4200) as shown in Table 4. I-V characteristics curve is plotted for various LO-doped chitosan films. The resistance of the LO-doped chitosan film is estimated from the slope of the I-V curve and resistivity has been calculated using the following relation.

$$\sigma = 1/\rho = (R \times t)/A \quad (2)$$

Where A is the area of the film, ρ is the resistivity of the sample, t is the thickness of the sample, and R is the resistance of the sample. The variation of the conductivity and surface roughness of the film with respect to variation LO is presented in Figure 5.

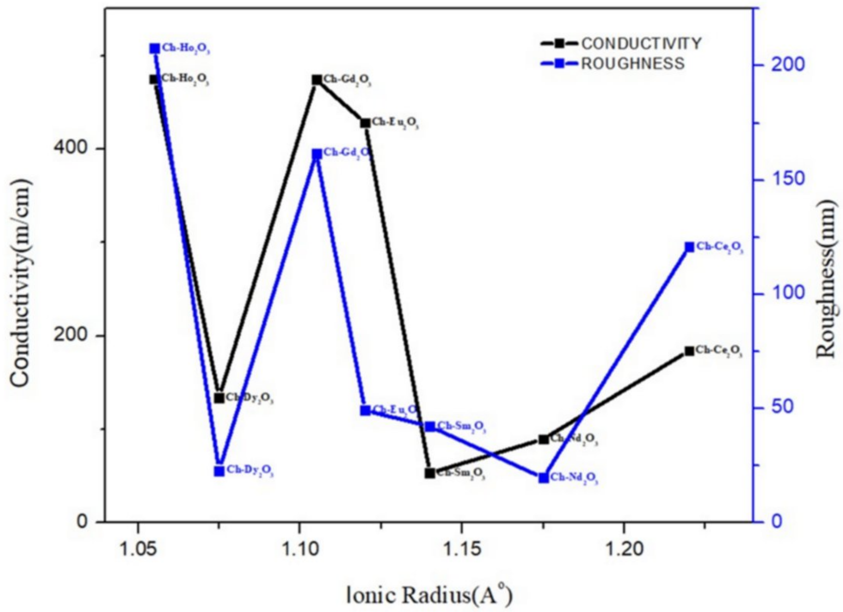

FIGURE 5: Conductivity vs roughness for various LO-doped chitosan films

LO, lanthanide oxide

Chemical formula	Ionic radius (Å)	Conductivity (μS/cm)	Roughness (nm)
Chitosan + Ce_2O_3	1.22	184	120.8
Chitosan + Nd_2O_3	1.175	89.7	19.7
Chitosan + Sm_2O_3	1.14	53.1	42.2
Chitosan + Eu_2O_3	1.12	428	49.2
Chitosan + Gd_2O_3	1.105	474	161.8
Chitosan + Dy_2O_3	1.075	134	22.9
Chitosan + Ho_2O_3	1.055	475	207.8

TABLE 4: Conductivity for various LO-doped chitosan film

LO, lanthanide oxide

Surface roughness has a greater impact on electrical conductivity when thin film thickness falls and approaches the mean free path of electrons. Surface roughness in this situation raises the electric resistance. The approach of Fishman and Calecki was applied to account for the universal power law that gives the equation of the variation of the film conductivity with increasing film roughness (d) [31]

$\sigma = d^c$ (3)

The result of roughness versus conductivity of the Ch-LO film is well in agreement with the above Fishman and Calecki equation. The interface scattering is based on the roughness of thin films. Because of the surfaces generally have smooth properties across all length scales, there is a higher conductivity and stronger quantum mechanical effects [32].

Discussion

The discussion section presents the results of this research in terms of previous research on chitosan-based composites and doping with LOs. The main points which support this are given below:

Chemical interactions and structural changes

The FTIR result validating successful integration of LOs into the chitosan matrix is consistent with earlier research on chitosan-based composites. For example, the shifts in peak positions for N-H, amine, C-H, and C-N groups observed are in agreement with results from research on chitosan-LO nanocomposites [33].

Improved optical properties

The remarkable increase in PL intensity, especially for the samarium-doped film, supports earlier studies of rare earth doped compounds for use in LEDs [26]. This supports the increasing demands for lanthanide-doped materials due to their interesting optical properties.

Morphological characteristics and surface roughness

Variations in surface morphology and roughness on LO doping, as noted, are similar to research work on chitosan-based piezoelectric composite thin films [34]. The variation in observed roughness values (28.9 nm in Dy_2O_3-doped to 264 nm in Ho_2O_3-doped chitosan) gives new knowledge regarding the effect of various LOs on surface properties.

Correlation between electrical conductivity and surface roughness

The Fishman and Calecki model correlate the surface roughness and electrical conductivity as cited in the research. It corresponds to studies regarding the impact of the surface roughness on electrical conductivity in thin films [31,32,39].

Implications for material design and applications

The debate on possible uses of these materials in bioelectronics, pollution remediation, and high-end materials science is commensurate with the general research trend on chitosan-based composites. For instance, the increased conductivity in Gd_2O_3 and Ho_2O_3-doped samples is applicable to the fabrication of bio-compatible electronic interfaces, and the studies on chitosan-ZnO nanocomposites in vibration sensors [14].

Conclusions

The chitosan-based LO has been synthesized successfully and the films were taken into different characterization. The FTIR studies confirm the presence of the functional group, and shifts found in the spectra confirm the doping of different LO with chitosan. The surface topography and roughness of all the samples are analyzed by AFM. From the AFM, it is confirmed that the variation of roughness is influenced by the doping of different LOs. The roughness is high for the chitosan-based Ho_2O_3 and less for the chitosan-based Dy_2O_3, with the values being respectively 264 nm and 28.9 nm. From the PL spectra, the emission peaks are observed in the range between 500 and 550 nm for all samples with different intensities where the intensity was high for pure chitosan, and a change in intensity was found for the Ch-LO. The conductivity of chitosan doped with different LOs has been studied using the Keithley Source meter. The conductivity is high for the Gd_2O_3 and Ho_2O_3, whereas the other chitosan-based oxides have less conductivity, aligning with the studies by JK (2021), Shiri and Ehsani (2016). The doping of LOs enhances the conductivity of chitosan in comparison with pure chitosan. The surface roughness of the film is directly proportional to the conductivity of the same.

The recognition of the necessity of continued research on concentration-dependent effects and targeted applications reflects the iterative process of materials science research. This methodology is in line with other field investigations that are calling for deeper investigation into the mechanisms of charge transport and application-dependent optimization. Overall, the argument does a good job of situating the research findings in relation to what is currently known on chitosan composites and LO doping, as well as how this research makes new contributions to the field.

Additional Information

Author Contributions

All authors have reviewed the final version to be published and agreed to be accountable for all aspects of the work.

Concept and design: Chinnan Raja Mohan, Kabiriyel J., Shanmugaprakash R.

Acquisition, analysis, or interpretation of data: Chinnan Raja Mohan, Kabiriyel J., Padma M.J., Jeyanthi R., Shanmugaprakash R.

Drafting of the manuscript: Chinnan Raja Mohan, Kabiriyel J., Padma M.J., Jeyanthi R., Shanmugaprakash R.

Critical review of the manuscript for important intellectual content: Chinnan Raja Mohan, Kabiriyel J., Shanmugaprakash R.

Supervision: Chinnan Raja Mohan, Shanmugaprakash R.

Disclosures

Human subjects: All authors have confirmed that this study did not involve human participants or tissue. **Animal subjects:** All authors have confirmed that this study did not involve animal subjects or tissue. **Conflicts of interest:** In compliance with the ICMJE uniform disclosure form, all authors declare the following: **Payment/services info:** All authors have declared that no financial support was received from any organization for the submitted work. **Financial relationships:** All authors have declared that they have no financial relationships at present or within the previous three years with any organizations that might have an interest in the submitted work. **Other relationships:** All authors have declared that there are no other relationships or activities that could appear to have influenced the submitted work.

References

1. Dash M, Chiellini F, Ottenbrite RM, Chiellini E: Chitosan—a versatile semi-synthetic polymer in biomedical applications. Progress in Polymer Science. 2011, 36:981-1014. 10.1016/j.progpolymsci.2011.02.001
2. Mohan CR, Kandasamy R, Kabiriyel J: Correlation between electrical conductivity and antibacterial activity of chitosan-stabilized copper and silver nanoparticles. Carbohydrate Polymer Technologies and Applications. 2024, 7:100503. 10.1016/j.carpta.2024.100503
3. Mohan CR, Murugan S, Jayakumar K: Conductivity study of chitosan based nanocomposites. AIP Conference Proceedings. 2012, 1447:205-6. 10.1063/1.4709952
4. Mohan CR, Gowrisankar A, Uthayakumar R, Jayakumar K: Morphology dependent electrical property of chitosan film and modeling by fractal theory. The European Physical Journal Special Topics. 2019, 228:233-43. 10.1140/epjst/e2019-800113-4
5. Mohan CR, Senthilkumar M, Jayakumar K: Conductivity studies of Chitosan doped with different ammonium salts: effect of ion size. AIP Conference Proceedings. 2015, 1665:040012. 10.1063/1.4917625
6. Mohan CR, Sathya R, Nithiananthi P, Jayakumar K: Ultrasonic velocimetry studies on different salts of chitosan: effect of ion size. International Journal of Biological Macromolecules. 2017, 104:1596-603. 10.1016/j.ijbiomac.2017.02.049
7. Jayakumar R, Prabaharan M, Nair SV, Tamura H: Novel chitin and chitosan nanofibers in biomedical applications. Biotechnology Advances. 2010, 28:142-50. 10.1016/j.biotechadv.2009.11.001
8. Farzana MH, Meenakshi S: Exploitation of zinc oxide impregnated chitosan beads for the photocatalytic decolorization of an azo dye. International Journal of Biological Macromolecules. 2015, 72:900-10. 10.1016/j.ijbiomac.2014.09.038
9. Prabhu SM, Meenakshi S: A dendrimer-like hyper branched chitosan beads toward fluoride adsorption from water. International Journal of Biological Macromolecules. 2015, 78:280-86. 10.1016/j.ijbiomac.2015.04.002
10. Farzana MH, Meenakshi S: Synergistic effect of chitosan and titanium dioxide on the removal of toxic dyes by the photodegradation technique. Industrial & Engineering Chemistry Research. 2013, 53:55-63. 10.1021/ie402347g
11. Prabhu SM, Elanchezhiyan SSD, Lee G, Meenakshi S: Defluoridation of water by tea-bag model using La3+ modified synthetic resin@chitosan biocomposite. International Journal of Biological Macromolecules. 2016, 91:1002-9. 10.1016/j.ijbiomac.2016.05.112
12. Prokhorov E, Luna-Bárcenas G, González-Campos JB, Kovalenko Y, García-Carvajal ZY, Mota-Morales J: Proton conductivity and relaxation properties of chitosan-acetate films. Electrochimica Acta. 2016, 215:600-8. 10.1016/j.electacta.2016.08.148
13. Praveen E, Murugan S, Jayakumar K: Nano ZnO embedded in Chitosan matrix for vibration sensor application. AIP Conference Proceedings. 2015, 1665:050032. 10.1063/1.4917673
14. Praveen E, Murugan S, Jayakumar K: Investigations on the existence of piezoelectric property of a bio-polymer - chitosan and its application in vibration sensors. RSC Advances. 2017, 7:35490-495. 10.1039/c7ra04752e
15. Du L, Li T, Jin F, et al.: Design of high conductive and piezoelectric poly (3,4-ethylenedioxythiophene)/chitosan nanofibers for enhancing cellular electrical stimulation. Journal of Colloid and Interface Science. 2019, 559:65-

75. 10.1016/j.jcis.2019.10.003

16. Praveen E, John Peter I, Muthu kumar A, Ramachandran K, Jayakumar K: Performance of ZnO/ZnS nanocomposite based dye-sensitized solar cell with chitosan-polymer electrolyte. Materials Today Proceedings. 2021, 35:27-30. 10.1016/j.matpr.2019.05.382
17. Kabiriyel J, Raja Mohan C: "Size or mass" which plays a role? An investigation on the optical and ultrasonic properties of chitosan-lanthanide composites. International Journal of Biological Macromolecules. 2021, 188:609-19. 10.1016/j.ijbiomac.2021.08.050
18. Jeyanthi, R, Kabiriyel, J, & Raja Mohan, C: Effect of ion size on the thermodynamical properties of different salts of chitosan. Journal of Pure and Applied Ultrasonics,. 2021, 43:2.
19. Mohan CR, Manikandan R, Jayakumar K: An unusual behavior on the electrical properties of various salts of chitosan. AIP Conference Proceedings. 2014, 1591:172-74. 10.1063/1.4872533
20. Mohan CR, Murugan S, Nithiananthi P, Jayakumar K: Effect of ion size of various salts of Chitosan on the electrical properties. AIP Conference Proceedings. 2013, 1536:405-6. 10.1063/1.4810272
21. Kabiriyel J, Jeyanthi R, Jayakumar K, et al.: Green synthesis of carboxy methyl chitosan based curcumin nanoparticles and its biological activity: Influence of size and conductivity. Carbohydrate Polymer Technologies and Applications. 2023, 5:100260. 10.1016/j.carpta.2022.100260
22. Cho YW, Cho YN, Chung SH, Yoo G, Ko SW: Water-soluble chitin as a wound healing accelerator. Biomaterials. 1999, 20:2139-45. 10.1016/s0142-9612(99)00116-7
23. El Sayed AM, Mohamad ADM: Synthesis, structural, thermal, optical and dielectric properties of chitosan biopolymer; influence of PVP and α-Fe2O3 nanorods. Journal of Polymer Research. 2018, 25:1-14. 10.1007/s10965-018-1571-x
24. Huang X, Li LD, Lyu GM, et al.: Chitosan-coated cerium oxide nanocubes accelerate cutaneous wound healing by curtailing persistent inflammation. Inorganic Chemistry Frontiers. 2018, 5:386-93. 10.1039/c7qi00707h
25. Divina R, Teresa PE, Marimuthu K: Dy3+ ion as optical probe to study the luminescence behavior of alkali lead bismuth borate glasses for w-LED application. Journal of Alloys and Compounds. 2021, 883:160845. 10.1016/j.jallcom.2021.160845
26. Divina R, Naseer KA, Marimuthu K, Alajerami YSM, Al-Buriahi MS: Effect of different modifier oxides on the synthesis, structural, optical, and gamma/beta shielding properties of bismuth lead borate glasses doped with europium. Journal of Materials Science Materials in Electronics. 2020, 31:21486-501. 10.1007/s10854-020-04662-3
27. Hassannejad H, Nouri A: Synthesis and evaluation of self-healing cerium-doped chitosan nanocomposite coatings on AA5083-H321. International Journal of Electrochemical Science. 2016, 11:2106-118. 10.1016/s1452-3981(23)16086-x
28. Blasse G: Luminescence of rare earth ions at the end of the century. Journal of Alloys and Compounds. 1993, 192:17-21. 10.1016/0925-8388(93)90172-j
29. Zhang J, Li Y, Hao X, et al.: Recent progress in therapeutic and diagnostic applications of lanthanides.. Mini-Reviews in Medicinal Chemistry. 2011, 11:678-94. 10.2174/138955711796268804
30. Rinaudo M: Chitin and chitosan: properties and applications. Progress in Polymer Science. 2006, 31:603-32. 10.1016/j.progpolymsci.2006.06.001
31. Javidjam A, Hekmatshoar MH, Hedayatifar L, Abad SNK: Effect of surface roughness on electrical conductivity and hardness of silver plated copper. Materials Research Express. 2018, 6:036407. 10.1088/2053-1591/aaf4c5
32. Palasantzas G, Barnaś J: Surface-roughness fractality effects in electrical conductivity of single metallic and semiconducting films. Physical Review B. 1997, 56:7726-731. 10.1103/physrevb.56.7726
33. Bashal AH, Khalafalla M, Abdel-Basset TA: Dielectric properties and AC conductivity of chitosan-La2O3 nanocomposite. Arabian Journal for Science and Engineering. 2020, 46:5859-64. 10.1007/s13369-020-04958-w
34. Zidani J, Zannen M, Da Costa A, et al.: Investigation of microstructure and physical characteristics of eco-friendly piezoelectric composite thin films based on chitosan and Ln2O3-doped Na0.5Bi0.5TiO3-BaTiO3 nanoparticles. Nanomaterials. 2024, 14:1755. 10.3390/nano14211755
35. Prokhorov E, Luna-Bárcenas G, Limón JMY, Sanchez AG, Kovalenko Y: Chitosan-ZnO nanocomposites assessed by dielectric, mechanical, and piezoelectric properties. Polymers. 2020, 12:1991. 10.3390/polym12091991
36. Ayhan NK, Torgut G: Structural, dielectric, and electrical properties of chitosan composites doped with silver for electrochemical applications. ChemistrySelect. 2024, 9:e202404348. 10.1002/slct.202404348
37. Domyati D: Dielectric and optoelectronics properties of thin films based on chitosan containing titanium oxide/hematite and their potential for optoelectronics devices. Journal of Materials Science Materials in Electronics. 2024, 35:1-13. 10.1007/s10854-024-12102-9
38. Bhatt AS, Bhat DK, Santosh MS, Tai CW: Chitosan/NiO nanocomposites: a potential new dielectric material. Journal of Materials Chemistry. 2011, 21:13490-497. 10.1039/c1jm12011e
39. Ketenoglu D, Ünal B: Influence of surface roughness on the electrical conductivity of semiconducting thin films. Physica A Statistical Mechanics and its Applications. 2013, 392:3008-17. 10.1016/j.physa.2013.03.007